Micromachines **2010**, *1*, 36-47; doi:10.3390/mi1020036

OPEN ACCESS

micromachines

ISSN 2072-666X

www.mdpi.com/journal/micromachines

Article

Analysis of Electrokinetic Mixing Techniques Using Comparative Mixing Index

Mranal Jain [1,*], Anthony Yeung [1] and Krishnaswamy Nandakumar [2]

1 Department of Chemical and Materials Engineering, University of Alberta, Edmonton, AB, Canada; E-Mail: tony.yeung@ualberta.ca

2 Cain Department of Chemical Engineering, Louisiana State University, Baton Rouge, LA 70803, USA; E-Mail: nandakumar@lsu.edu

* Author to whom correspondence should be addressed; E-Mail: mjain@ualberta.ca; Tel.: +1-780-993-7366; Fax: +1-780-492-2881.

Received: 9 March 2010; in revised form: 19 May 2010 / Accepted: 2 July 2010 / Published: 12 July 2010

Abstract: The performance of micro-mixers is evaluated in terms of deviations from perfectly mixed state and mixing length (*i.e.*, device length required to achieve perfect mixing). Different variations of T-mixer are reported for improved mixing performance, including geometric constrictions/obstacles embedded in the channel wall, heterogeneously charged walls, grooves on channel base, *etc*. Most of the reported designs provide improved mixing at the expense of reduced flow rate; there exists therefore a tradeoff between mixing and transport. The reduced flow rate, which affects species residence time, is unfortunately not taken into account in most micro-mixing performance analyses. This issue is addressed by the comparative mixing index (CMI), which evaluates mixing performance more appropriately by normalizing the effect of residence time among different designs. In this study, the performance of several mixing strategies are evaluated based on the CMI; these are mixer designs that incorporate (a) physical constrictions, (b) induced charge electro-osmotic (ICEO) effects, and (c) heterogeneously charged walls. The present analysis clearly identifies conditions under which a given mixer design is superior to a T-mixer.

Keywords: micro-mixer; micro-fluidics; mixing index

---

1. Introduction

Micro-mixers are often a critical component of miniaturized diagnostic devices, as mixing is essential for fast analysis in many applications (e.g. biochemical analysis, complex enzyme reactions, *etc*.). Under practically all operating conditions, fluid flow in a micro-device is in the laminar regime. Such low Reynolds number flows are, by nature, very difficult to mix; the predominant mechanism of equalizing concentration differences is therefore often relegated to diffusion. However, mixing designs do exist in miniaturized devices; such micro-mixers can be categorized as either active or passive [1]. Active mixers utilize external energy—via pressure, electro-kinetic disturbance, *etc*.—to induce transverse flows. On the other hand, diffusion and chaotic advection are the dominant mixing mechanisms in passive mixers. An excellent review of electro-kinetic mixing techniques [2] and various micro-mixer types, along with their comparisons, can be found elsewhere [1].

The most basic type of passive micro-mixer is a T- or Y-mixer, where two confluent streams intermix due to transverse diffusion. Various modifications have been reported in the literature for enhancing mixing performance of such mixers. Some of these approaches include: sequential injection of samples [3], patterned heterogeneous surface charge along the channel bottom [4], grooved patterns on the channel base [5], instability mixing due to electrical conductivity gradients [6], and the use of embedded conducting [7–10] or non-conducting [11,12] obstacles within the microchannel. Typically, such designs provide effective mixing either by reducing the diffusion length or by increasing the interfacial contact area for mass transfer within the microchannel. The mixing performance is further augmented by the reduced flow rate [7–12] of such designs, which increases the species residence time within the micro-device. While an increased interfacial contact area or shortened diffusion length is favored in any improved design, mixing enhancement due to residence time effect is often not desirable. Therefore, it is important to normalize the effect of residence time when comparing different micro-mixer designs. Although many studies have noted the reduced flow rates for improved mixer designs [2,10,13], the residence time effect has not been taken into consideration in micro-mixing performance evaluation. Most of the reported studies evaluate micro-mixers based on departures from perfectly mixed state [7–12] or from the length required to achieve perfect mixing. Recently, a comparative mixing index (CMI) was proposed for characterization and comparative analysis of micro-mixers [14]. For a given design, the CMI evaluates the mixing performance at similar residence time (as for T-mixer) and hence identifies the 'true' non-diffusive mixing improvement for any given design over a T-mixer. In this study, several electrokinetic mixing designs, namely, (a) physical constriction mixer, (b) induced charge electro-osmotic (ICEO) mixer, and (c) heterogeneously charged wall mixer, are analyzed using the comparative mixing index. The organization of this article is as follows: the following section introduces the comparative mixing index (CMI) for micro-mixing characterization. The next section describes the mathematical model used for simulating electrokinetically driven micro-mixers. In results section, CMI-based analyses of different micro-mixers are presented; this will be followed by the conclusions.

2. Comparative Mixing Index (CMI)

The most commonly used performance index for micro-mixers evaluates the departure from the perfectly mixed state [7–12]; the associated mixing index η is defined as

$$\eta = \left[1 - \frac{\sqrt{\frac{1}{N}\sum_{1}^{N}\left(\bar{c}_s - \bar{c}_s^*\right)^2}}{\sqrt{\frac{1}{N}\sum_{1}^{N}\left(\bar{c}_s^0 - \bar{c}_s^*\right)^2}} \right] \tag{1}$$

In the above equation, N is the number of points in the cross-section used for estimation of the mixing index. The variable $\bar{c}_s$ represents the scaled concentration value at that point, while $\bar{c}_s^0$ and $\bar{c}_s^*$ are the scaled concentrations at each location if the solutions were unmixed and perfectly mixed (*i.e.* $\bar{c}_s^* = 0.5$), respectively. It should also be noted that the variable $\bar{c}_s^0$ takes on the value of 0 or 1 at any location across the channel width, resulting in a constant denominator value of 0.5 in Equation 1. Based on the definition of the mixing index (Equation 1), the theoretical range for η is between zero and one. Typically, the above index is evaluated at the channel exit and it has been extensively employed for comparative analysis between various micro-mixer designs. As stated earlier, the mixing index η does not account for reduced flow rates or variations in the residence time τ among different designs.

The comparative mixing index (CMI) evaluates any two arbitrary mixers of same residence time [14]. For any two designs A and B, the CMI can be defined as follows:

$$\alpha_{A,B} = \frac{(\eta)_A\big|_{(L_c,\tau)}}{(\eta)_B\big|_{(L_c,\tau)}} \tag{2}$$

If any design A is evaluated against the T-mixer, the above index can be written as:

$$\alpha_{A,\,T-mixer} = \frac{(\eta)_A\big|_{(L_c,\tau)}}{(\eta)_{T-mixer}\big|_{(L_c,\tau)}} \tag{3}$$

Based on the mixing index definition (Equation 3), the theoretical limits for $\alpha_{A,T-mixer}$ is between one and infinity. It is apparent from the definition that the CMI normalizes the effect of residence time (flow rate) and identifies the true mixing improvement. For a given design A, values of CMI close to unity indicates equivalency to the T-mixer, whereas higher values suggest better mixing performance in comparison to the T-mixer. Also, the term $\alpha_{A,\,T-mixer} - 1$ identifies the non-diffusive mixing component for design A.

3. Mathematical Model

The non-conducting channel walls are assumed negatively charged with fixed zeta potential ς_f. The solution is treated as an incompressible Newtonian fluid with constant dielectric constant ε_r, viscosity μ, and density ρ. To describe the mathematical model, we introduce the following reference quantities and dimensionless variables:

$$L_{\text{ref}} = W, \quad \psi_{\text{ref}} = \frac{k_{\text{B}}T}{e}, \quad c_{\text{ref}} = c_{0,} \quad E_{\text{ref}} = \frac{\psi_{\text{ref}}}{L_{\text{ref}}}, \quad u_{\text{ref}} = \frac{\varepsilon_0\varepsilon_r\psi_{\text{ref}}}{\mu}E_{\text{ref}}, \text{ and}$$

$$\bar{x} = \frac{x}{L_{\text{ref}}}, \quad \bar{y} = \frac{y}{L_{\text{ref}}}, \quad \bar{\psi} = \frac{\psi}{\psi_{\text{ref}}}, \quad \bar{u} = \frac{u}{u_{\text{ref}}}, \bar{E} = \frac{E}{E_{\text{ref}}}, \quad \bar{p} = \frac{p}{\rho u_{\text{ref}}^2}, \quad \bar{t} = \frac{t u_{\text{ref}}}{L_{\text{ref}}}$$

Here W is the channel width, k_{B}, T, e, c_0 and ε_0 represent the Boltzmann constant, absolute temperature, electronic charge, species concentration and permittivity of free space, respectively. Other notations/symbols and simulation parameters used in this study are listed in Table 1.

Table 1. Simulation Parameters (default values).

Parameter	Value	Description
W	100 μm	Width of the microchannel
L_c	2 mm	Length of microchannel
ς_f	−50 mv	Fixed zeta potential on channel walls
D_s	5e−11 m^2/s	Diffusivity of species to be mixed
a	25 μm	Radius of non-conducting obstacle (Figure 2)
p	100 μm	Heterogeneous charged surface patch length (Figure 5)

With the assumption of thin electric double layer (EDL) and uniform bulk conductivity, the electric potential (ψ) distribution at steady state can be obtained by solving the Laplace equation. In its non-dimensional form, the Laplace equation is

$$\bar{\nabla}^2 \bar{\psi} = 0 \tag{4}$$

At the channel inlet, a constant potential V_0 relative to the outlet potential is applied, giving rise to a constant electric field E in the x direction. The normal component of electric field is specified as zero *i.e.* $n.\nabla\psi = 0$ at the channel wall and the obstacle surface.

The flow field in the computational domain is governed by the continuity and Navier-Stokes equations. These equations, in their dimensionless forms, are

$$Re(\bar{u} \cdot \bar{\nabla}\bar{u}) = -\bar{\nabla}\bar{p} + \bar{\nabla}^2\bar{u} \tag{5a}$$

$$\bar{\nabla} \cdot \bar{u} = 0 \tag{5b}$$

In the above equations, Re is the Reynolds number (ratio of inertial to viscous forces). The slip velocity boundary condition (Hemholtz-Smoluchowski's equation) is used to account for the electrical body force term as shown below [15]:

$$\bar{u} = \bar{\varsigma}\,\bar{E} \quad \text{where} \begin{Bmatrix} \bar{\varsigma} = \bar{\varsigma}_f \text{ at non-conducting surface} \\ \bar{\varsigma} = \bar{\varsigma}_i \text{ at conducting surface} \end{Bmatrix} \tag{6}$$

In the above equation, ς_f is the constant zeta potential on the non-conducting surface, while ς_i is the induced zeta potential (for ICEO mixer) on the conducting surface. The induced zeta potential is estimated using the correction method [7], (described later in the ICEO mixer section). The Smoluchowski slip condition (Equation 6) is imposed at fluid-solid boundaries, while zero pressure boundary conditions are imposed at the inlet and the outlet.

The steady transport of species is governed by the convection-diffusion equation; it can be written in terms of the Peclet number Pe as

$$Pe(\bar{u} \cdot \bar{\nabla}\bar{c}) = \bar{\nabla}^2\bar{c} \tag{7}$$

For species transport, a constant concentration condition is imposed at the channel inlets (*i.e.*, scaled concentrations of 1 and 0 at inlet 1 and inlet 2, respectively). The aforementioned condition is implemented at the inlet boundary using a smoothed Heaviside function (with continuous second derivatives). At the conducting surfaces and non-conducting channel walls, the zero flux condition is imposed for the species, while the convective-flux-only boundary condition is applied at the channel outlet. The above model is solved using the direct (UMFPACK) solver available within the commercial finite element method package, COMSOL 3.4. The numerical analysis is carried out with sufficiently fine mesh and the reported numerical results are shown to be mesh-independent.

4. Results and Discussion

The proposed index is used for characterization of the following mixer types: (1) physical constriction or obstacle based micro-mixer, (2) conducting obstacle or induced charge electro-osmotic (ICEO) mixer, and (3) heterogeneously charged walls mixer. The design schematic for the above mentioned micro-mixer types are shown in Figure 1.

Figure 1. Micro-mixer design schematic for (a) Physical constriction mixer (characterized by fixed zeta potential ς_f); (b) ICEO mixer (characterized by induced zeta potential ς_i on conducting obstacle surface) and (c) Heterogeneously charged wall mixer (staggered arrangement, characterized by heterogeneous zeta potential ς_{hetero} on heterogeneous patch).

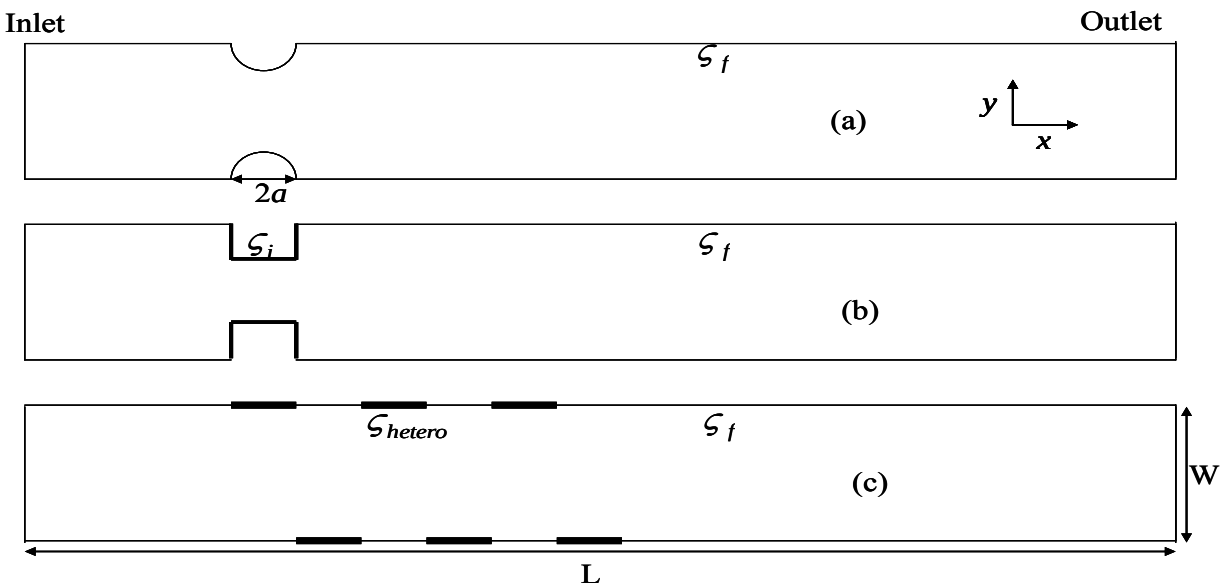

4.1. Physical Constriction / Obstacle Based Mixer

Mixing performance can be enhanced by introducing non-conducting obstacles embedded on the micro-channel wall [11,12]. It is shown that such obstacles/physical constrictions can reduce the diffusion length around the obstacle, which in turn enhances mixing. However, at the same time, these obstacles offer hydraulic resistance to flow and reduce the overall flow rate. In this study, a micro-mixer with a pair of non-conducting semi-cylindrical obstacle (radius a) is analyzed (Figure 1a). The

effect of obstacle radius on mixing performance is shown in Figure 2. The estimated CMI values are close to unity (see Figure 2), which indicates that physical constriction-type mixers do not offer any significant mixing benefits as compared to the T-mixer. The CMI analysis suggests that any increase in diffusive flux (due to obstacle) is offset by the additional flow resistance caused by the obstacle. The mixing performance does not increase appreciably with the number of obstacle pairs, as shown in Figure 3. However, mixing performance can be improved with heterogeneously charged obstacles [11,12], where micro-vortices can be generated in the microchannel due to surface heterogeneity.

Figure 2. Comparative mixing index (CMI) is plotted for physical constriction mixer for different obstacle radii.

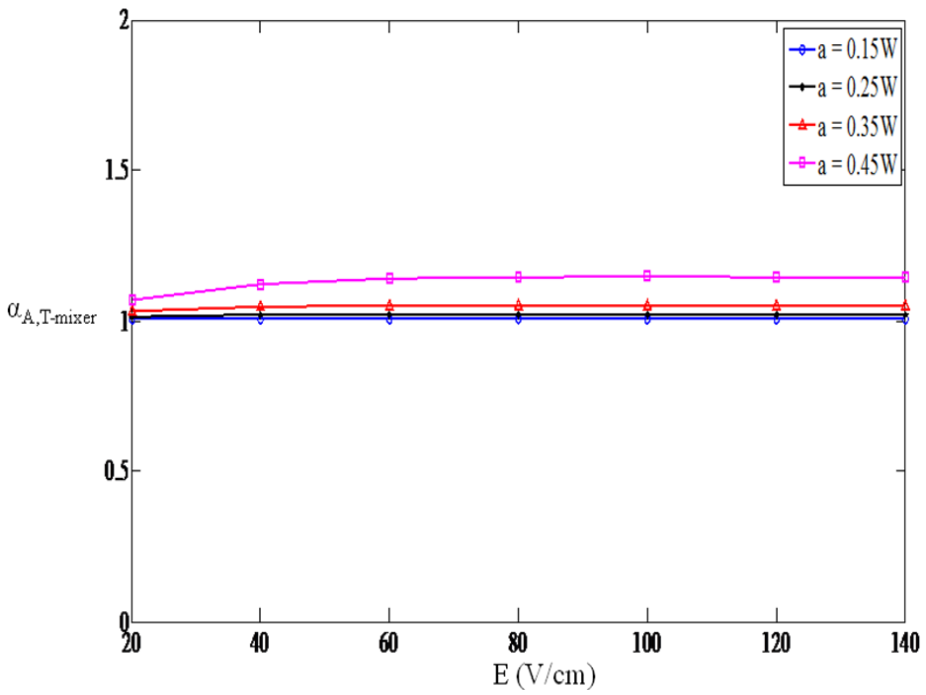

Figure 3. CMI plot for physical constriction mixer for different number of obstacle pairs, with $a = 0.25\ W$. The maximum CMI value is 1.15 (for N = 7).

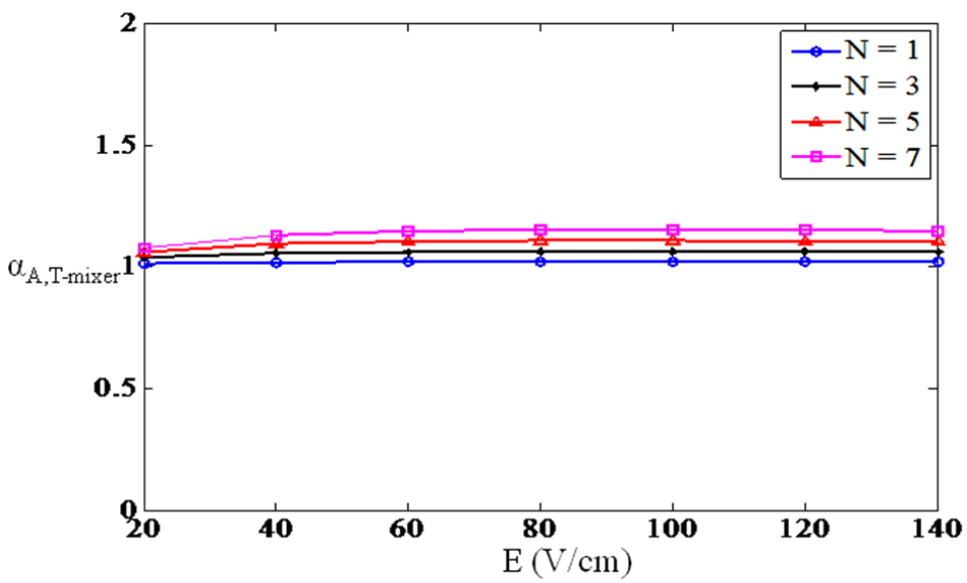

4.2. Induced Charge Electro-osmotic (ICEO)/ Conducting Obstacle Mixer

Conducting obstacle-based mixers are also known as induced charge electro-osmotic (ICEO) mixers, as charges are induced on polarizable and electrically conducting surfaces by an externally applied electric field [16]. Due to the induced charges, flow circulations are generated near the obstacle which enhances micro-mixing [7–10]. The design schematic for ICEO mixer with rectangular conducting obstacle is shown in Figure 1b. The most critical parameter for ICEO mixers is the induced charge/induced zeta potential ς_i. The magnitude of ς_i is dependent on the applied electric field, as well as the obstacle size and shape. In this study, steady state induced zeta potential is estimated using the Correction method [7] based on the following equations:

$$\bar{\varsigma}_i = -\bar{\psi} + \bar{\psi}_c \tag{8}$$

Here $\bar{\psi}_c$ is the constant correction potential, which can be estimated based on charge conservation on the conducting surface, *i.e.*

$$\psi_c = \frac{\int_s \psi \, dA}{A} \tag{9}$$

In the above equation, A represents the surface area of the conducting obstacle.

In Figure 4a, the CMI is plotted for semi-cylindrical conducting obstacles with $a = 0.2\,W$ and $a = 0.4\,W$. The magnitude of the induced potential increases with the obstacle radius which in turn increases the ICEO transverse flow in the microchannel, resulting in better mixing as compared to T-mixer (Figure 4a). The corresponding η values are plotted for an ICEO mixer ($a = 0.4\,W$) and a T-mixer in Figure 4b. It is evident from the CMI and η plots (Figure 4) that ICEO mixers provide better mixing compared to T-mixers. The primary reason for enhanced mixing is the generation of micro-vortices due to induced charge electrokinetic flow. Moreover, the induced transverse ICEO velocity scales quadratically with respect to electric field resulting in superior mixing performance at higher fields [7–10]. Next, we investigate the effect of obstacle shape on mixing performance. Previous study [10] has identified 'right triangle' as an optimal shape for maximizing mixing performance in ICEO mixers. The rectangular shape and the optimal shape (right triangle) are examined for a range of electric field values. As reported earlier [10], the η plot (Figure 5a) suggests that the right-triangle shape obstacle provides better mixing than its rectangular counterpart. The reason for superior performance of the optimal shape is the increased species residence time. The optimal shape, due to its non-symmetric shape, reduces the overall flow rate by inducing ICEO back flow [10]. However as CMI normalizes the effect of residence time, the CMI values are higher for rectangular shape as demonstrated in Figure 5b. For the right-triangle shape, the CMI value approaches unity in the high field limit, resulting in equivalent mixing performance as for a T-mixer. Based on the η and CMI plots, the optimal range of operation for right-triangle shaped mixers appears to be between $E = 140$ and 180 V/cm.

Figure 4. (a) CMI plot for an ICEO mixer; mixing performance increases with conducting obstacle radius. (b) An ICEO mixer and a T-mixer are compared in terms of η values. Both the CMI and η plots suggest that the ICEO mixer provides superior mixing at higher electric fields compared to the T-mixer.

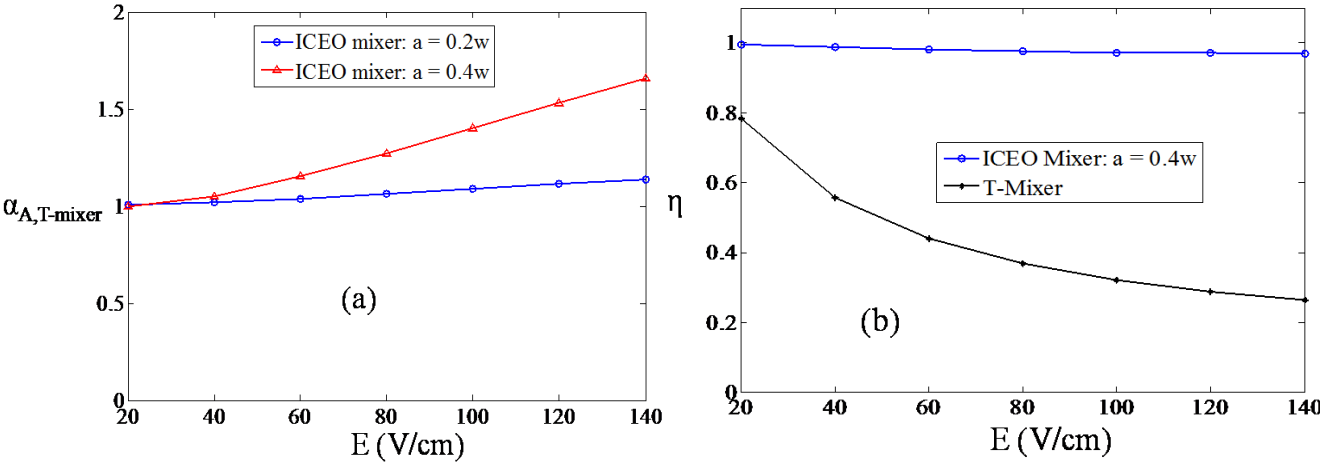

Figure 5. Rectangular shaped and optimally (right-triangle) shaped obstacles are examined using CMI and η plots for ICEO mixer. Although the η values suggest that the right-triangle shape provides superior mixing (5a), the CMI values are higher for the rectangular shape (5b). Upon further increase in electric field, the CMI values for the optimal shape will approach unity.

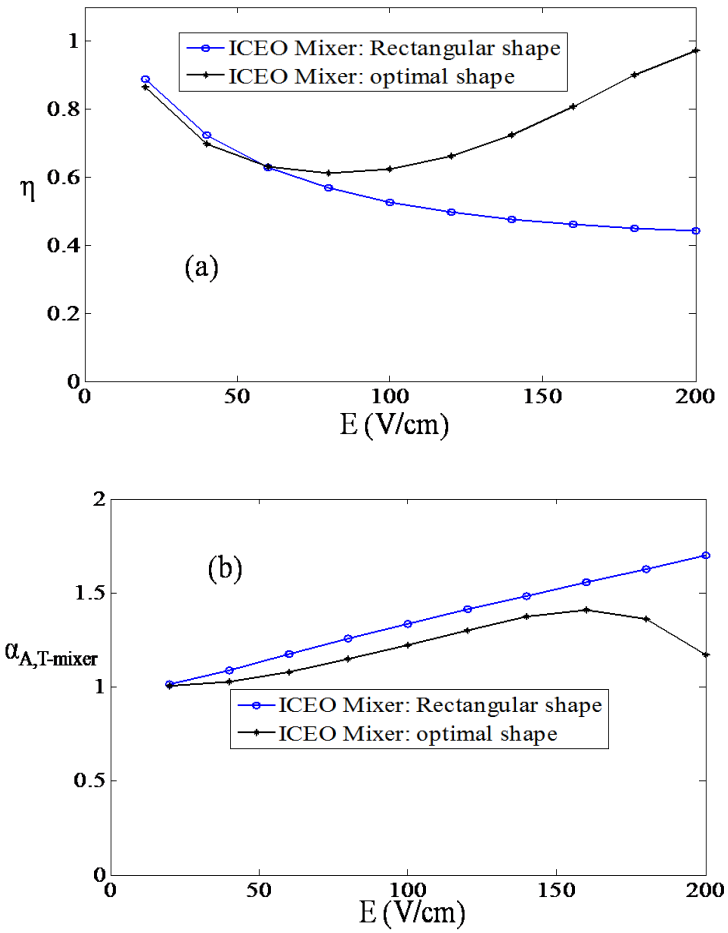

4.3. Heterogeneously Charged Walls Mixer

Heterogeneously charged patches can be used to generate flow circulations within a micro-channel; this in turn will enhance micro-mixing [13,17]. Theoretical analysis of such a phenomenon is carried out with heterogeneous patches on opposing walls. The patches are arranged in a staggered manner (Figure 1c), with opposing patches on the two walls having an offset that is equal to the patch length. (Here, N_p = number of patches, ς_{hetero} = zeta potential on the patch surfaces, L_p = length of each patch, which equals the channel width W). The mixing performance is examined for different ratios of zeta potential ($R = \varsigma_{hetero} / \varsigma_f$). The flow profile and species concentration surface plot are shown for different R values in Figure 6a. It can be seen that the size of the vortices (which relates to enhanced mixing) increases with negative values of R. The corresponding vorticity contour plots are shown in Figure 6b. The strength of flow circulations increases with the magnitude of heterogeneous zeta potential (higher negative R values) as suggested by Smoluchowski's equation (Equation 6).

Figure 6. (a) Species concentration surface plot and velocity arrow plot are shown for a mixer with heterogeneously charged walls (N_p = 3). The size of vortices increases with higher negative values of R, resulting in improved mixing. (b) Vorticity contours are plotted for equally spaced 100 points between −5000 to 5000 scaled values.

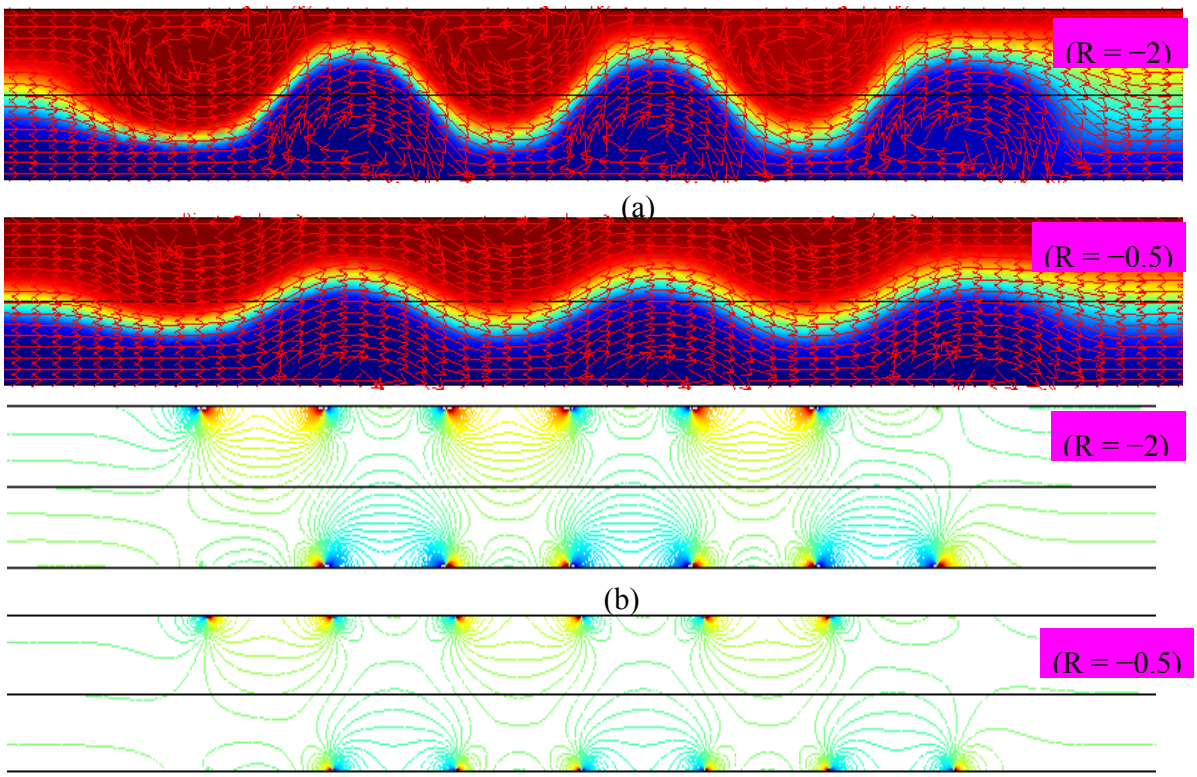

The CMI for various R values are plotted in Figure 7. In Figure 8a and 8b, η and CMI values are plotted for N_p = 3 and 6. Another interesting observation can be made with data points (Figure 8) corresponding to the electric field E = 40 V/cm. At this field strength, the η values suggest that the heterogeneously charged mixer (η = 0.96) is almost twice as good as the T-mixer (η = 0.55). However, for the same field strength, the CMI value is close to 1.1, which suggests similar mixing

performance for the two designs. This implies that flow circulations, at this electric field strength, does not cause considerable mixing (by reducing diffusion length) but rather reduces the flow rate significantly (by acting as flow resistance). It is therefore beneficial to operate such mixers at higher field strengths (E > 60 V/cm), as suggested by the results in Figure 8.

Figure 7. CMI plot for different ratios (denoted by R) of heterogeneous zeta potential to fixed zeta potential. The mixing performance increases with higher negative values of R.

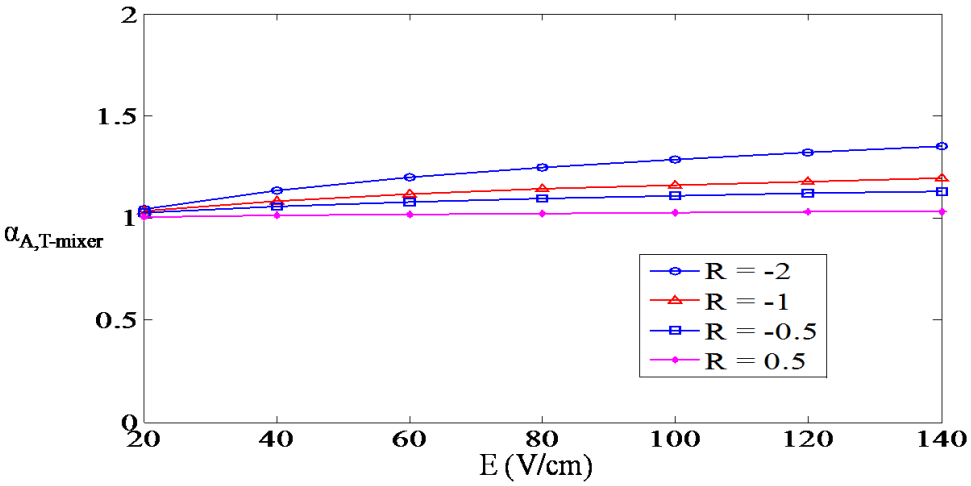

Figure 8. CMI and η values are plotted for heterogeneously charged wall mixers with $N_p = 3$ and $N_p = 6$. The mixing performance increases with the number of heterogeneous patches. For E = 40 V/cm, although the η values suggest superior mixing performance over the T-mixer (Figure 8a), the CMI values suggest only a marginal improvement over the T-mixer (Figure 8b).

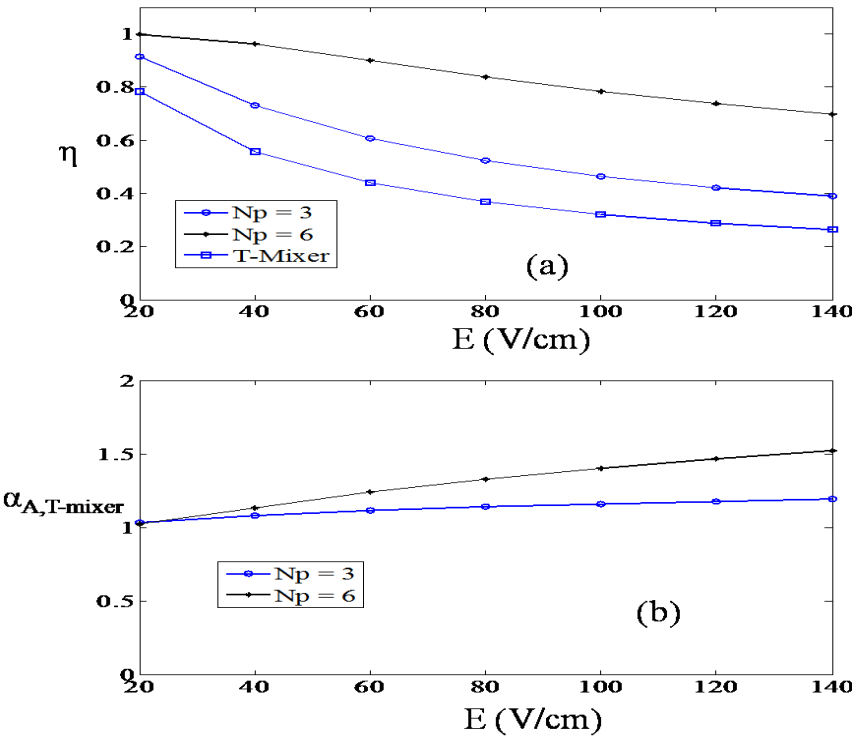

5. Conclusions

The comparative mixing index (CMI) is employed for analyzing three electrokinetic mixing designs: (a) physical constriction mixer, (b) ICEO mixer, and (c) heterogeneously charged walls mixer. As the CMI accounts for the species residence time (caused by reduced flow rate), it identifies the non-diffusive mixing improvement with respect to the T-mixer. Various case studies demonstrate the advantage of CMI over the existing mixing index (η), as the former reveals the conditions under which a given mixing strategy is advantageous over a T-mixer. It is also demonstrated that comparisons based solely on the parameter η are inadequate and may be misleading in terms of mixing improvement over the T-mixer (see Figures 4 and 7). The presented analysis can be extended to other mixing strategies and the CMI could be similarly useful for quantifying their performances.

References

1. Nguyen, N.T.; Wu, Z.G. Micromixers—A review. *J. Micromech. Microeng.* **2005**, *15*, R1–R16.
2. Chang, C.C.; Yang, R.J. Electrokinetic mixing in microfluidic systems. *Microfluid. Nanofluid.* **2007**, *3*, 501–525.
3. Coleman, J.T.; Sinton, D. A sequential injection microfluidic mixing strategy. *Microfluid. Nanofluid.* **2005**, *1*, 319–327.
4. Biddiss, E.; Erickson, D.; Li, D. Heterogeneous surface charge enhanced micromixing for electrokinetic flows. *Anal. Chem.* **2004**, *76*, 3208–3213.
5. Stroock, A.D.; Dertinger, S.K.W.; Ajdari, A.; Mezic, I.; Stone, H.A.; Whitesides, G.M. Chaotic mixer for microchannels. *Science* **2002**, *295*, 647–651.
6. Oddy, M.H.; Santiago, J.G.; Mikkelsen, J.C. Electrokinetic instability Micromixing. *Anal. Chem.* **2001**, *73*, 5822–5832.
7. Wu, Z.; Li, D. Mixing and flow regulating by induced-charge electrokinetic flow in a microchannel with a pair of conducting triangle hurdles. *Microfluid. Nanofluid.* **2008**, *5*, 65–76.
8. Wu, Z.; Li, D. Micromixing using induced-charge electrokinetic flow. *Electrochim. Acta* **2008**, *53*, 5827–5835.
9. Jain, M.; Yeung, A.; Nandakumar, K. Efficient micromixing using induced-charge electroosmosis. *J. Microelectromech. Syst.* **2009**, *18*, 376–384.
10. Jain, M.; Yeung, A.; Nandakumar, K. Induced charge electro osmotic mixer: Obstacle shape optimization. *Biomicrofluidics* **2009**, *3*, 022413.
11. Chang, C.C.; Yang, R.J. Computational analysis of electrokinetically driven flow mixing in microchannels with patterned blocks. *J. Micromech. Microeng.* **2004**, *14*, 550–558.
12. Chen, C.K.; Cho, C.C. Electrokinetically-driven flow mixing in microchannels with wavy surface. *J. Colloid Interface Sci.* **2007**, *3*, 470–480.
13. Tian, F.Z.; Li, B.M.; Kwok, D.Y. Tradeoff between mixing and transport for electroosmotic flow in heterogeneous microchannels with nonuniform surface potentials. *Langmuir* **2005**, *21*, 1126–1131.
14. Jain, M.; Nandakumar, K. Novel index for micromixing characterization and comparative analysis. *Biomicrofluidics* **2010**, in press.

15. Hunter, R.J. *Zeta Potential in Colloid Science: Principals and Applications*; Academic Press Inc.: New York, NY, USA, 1981.
16. Squires, T.M.; Bazant, M.Z. Induced-charge electro-osmosis. *J. Fluid Mech.* **2004**, *509*, 217–252.
17. Erickson, D.; Li, D. Influence of surface heterogeneity on electrokinetically driven microfluidic mixing. *Langmuir* **2002**, *18*, 1883–1892.